E-proceedings of the 38th IAHR World Congress
September 1-6, 2019, Panama City, Panama
doi:10.3850/38WC092019-0377

EXPERIMENTAL AND NUMERICAL STUDY ON WAVE-IMPACT ON BUILDINGS

DAVIDE WÜTHRICH[1], DAISUKE NISHIURA[2], SHUN NOMURA[3], MIKITO FURUICHI[4], MICHAEL PFISTER[5] & GIOVANNI DE CESARE[6]

[1,6] Platform of Hydraulic Constructions (PL-LCH), Ecole Polytechnique Fédérale de Lausanne (EPFL), Lausanne, Switzerland, d.wuthrich@uq.edu.au, giovanni.decesare@epfl.ch

[2,3,4] Department of Mathematical Science and Advance Technology (MAT), Japan Agency for Marine-Earth Science and Technology (JAMSTEC), Yokohama, Japan, nishiura@jamstec.go.jp, nomura.shun@jamstec.go.jp, m-furuic@jamstec.go.jp

[5] Civil Engineering Department, Haute Ecole d'Ingénierie et d'Architecture de Fribourg (HEIA-FR, HES-SO), Fribourg, Switzerland, michael.pfister@hefr.ch

ABSTRACT

Unsteady flows such as tsunamis, impulse waves and dam-break waves can lead to damages and human losses. Hence, specific research to limit casualties and reconstruction costs is needed. The complexity of the phenomena involved suggests that a hybrid experimental-numerical approach should be used to gain a more comprehensive understanding of the process. This paper presents an explorative study on the comparison of SPH numerical simulations using a highly effective parallel computing technique with large scale experimental data for dry bed surges and wet bed bores impacting free-standing buildings with and without openings. These preliminary results showed a relatively good agreement between the two approaches in the estimation of water depths around the buildings, which represents a key parameter for the design of vertical shelters. Nevertheless, some differences observed during the impact phase may be attributed to the incapability of the SPH numerical simulations to fully capture the turbulent nature of the process and its air-entrainment. These validation tests with detailed experimental data are a promising approach to improve the numerical models toward the development of reliable numerical tools for a safer design of resilient structures.

Keywords: SPH simulation, validation, tsunami, wave impact, inundation depths

1 INTRODUCTION

Tsunamis, impulse waves, dam-break waves and flood surges are rare, but catastrophic events, associated with high human losses and severe damages to infrastructures (Chock et al. 2012). At present, the estimation of wave-induced loads and inundation depths remains challenging, due to the complexity of the phenomena involved in the process. Despite numerous recent studies, a more accurate computation of these parameters is necessary for the design of safer infrastructures and reliable vertical shelters. Hence, a comprehensive understanding of the physical phenomenon based on a hybrid experimental-numerical approach is essential. The purpose of this research is to compare some experimental tests carried out at the Laboratory of Hydraulic Constructions (LCH) of Ecole Polytechnique Fédérale de Lausanne (EPFL) in Switzerland with a numerical model developed at the Department of Mathematical Science and Advance Technology (MAT) of the Japan Agency for Marine-Earth Science and Technology (JAMSTEC).

In literature, most previous studies are based on experimental approaches. The frontal impact on impervious free-standing buildings was widely investigated in the past and a variety of formulae was introduced to estimate wave-induced loads (Cross 1967, Ramsden 1993, Arnarson 2009, Nouri et al. 2010, Shafiei et al. 2016, Foster et al. 2017 and Wüthrich et al. 2018b, among others). In addition, previous studies pointed out that a specific design could reduce the impact forces exerted by the incoming wave on the buildings (Thusyanthan and Madabhushi 2008, Wilson et al. 2009). The presence of openings allowed for a flow through the buildings, decreasing the upstream water depths and increasing the downstream ones, resulting into a linear reduction of the maximum horizontal force, when compared to the corresponding impervious configuration (Triatmadja and Nurhasanah 2012, Wüthrich et al. 2018c). The scenario with building overtopping was shown to increase the downstream water depth, thus reducing the total load acting on the structure (Wüthrich et al. 2019). The orientation of the building also showed to have a key role in the loading process (Shafiei et al. 2016, Ylla Arbós et al. 2018).

In parallel with the experimental work, some numerical models based on computational fluid mechanics were developed to investigate tsunami-like flows (St-Germain et al. 2014, Crespo et al. 2015, Guler et al. 2018, Asadollahi 2018a, b). However, because of the complexity of the turbulent nature of free surface flows, most simulation studies were generally carried out for a simple flow structure in a small spatial domain. Only a few

studies addressed the issue of building impact from a numerical approach. The present study employs a *Smoothed Particle Hydrodynamics* (SPH) model (Monaghan, 1992). Contrarily to mesh-based methods, SPH is a particle-based method that can easily deal with free surface flows and splashing of water mass occurring during a tsunami impact on buildings. Although particle-based methods like SPH are suitable for simulating large scale phenomena with free surface flows, its high computational load represents an important limitation. For this, Nishiura et al. (2015) and Furuichi and Nishiura (2017) developed a SPH code for high-performance parallel computer system by using a dynamic load balancing technique. To simulate the impact of tsunami-like waves on buildings, 512 central processing unit nodes of the K super computer (RIKEN) in Kobe, Japan were used. This numerical model was previously validated to correctly reproduce the main hydrodynamic properties of tsunami-like waves (Nishiura et al. 2019). This study focuses on the validation of numerical simulations with large scale experimental set-up for the development of reliable damage-evaluation tools in case of wave-impact on free-standing structures.

Herein, the results derived from both numerical and experimental studies are applied to the fluid-structure interaction, resulting into a combined approach in the estimation of key parameters for the design of safer hydraulic structures in tsunami-prone areas. More specifically, the inundation depths upstream of buildings with different geometries are herein compared and discussed. This paper shows preliminary results showing that the SPH numerical simulations represent a good approach for a better understanding of the physical phenomenon and could thus be used for the design of safer resilient structures.

2 HYBRID APPROACH

The purpose of hybrid modelling is to combine aspects of both physical and numerical modelling for a more comprehensive understanding of all involved processes (Wüthrich et al. 2018d). This technical paper presents the physical modelling in Sect. 2.1 and the numerical modelling in Sect. 2.2.

2.1 Experimental set-up

All experimental tests were carried out in a large-scale facility at Laboratory of Hydraulic Constructions (LCH) of Ecole Polytechnique Fédérale de Lausanne (EPFL) in Switzerland. Waves were generated using a vertical release technique, similarly to Chanson et al. (2002), Meile et al. (2011), Rossetto et al. (2011) and Foster et al. (2017). Wüthrich et al. (2018a) showed that these waves had similar characteristics to the dam break waves, nowadays considered a better option than solitary waves to reproduce tsunami-like flows (Chanson 2006, Madsen et al. 2008). The vertical drop of a $7m^3$ volume from an upper reservoir into a lower basin generated wet bed bores and dry bed surges in the downstream channel (Figure 1). The released discharge was controlled by means of three identical pipes, independently operated, thus generating waves with different hydrodynamic properties (Wüthrich et al. 2018a). Both surges and bores propagate on a smooth horizontal channel with a length of 15.5 m and a width of 1.4 m. The roughness of the channel was estimated to a Darcy Weisbach friction factor f = 0.02 through detailed experiments under steady flow conditions.

A building was installed at a distance of 14.0 m from the channel inlet (Figure 1), represented by an aluminium cube of $B = H_B$ = 0.30 m. Based on a 1:30 Froude similitude, this corresponded to residential buildings of three floors (9 m), commonly observed in coastal areas subject to tsunami hazard. Initially only the impervious scenario was tested (P = 0 %), then 5 additional opening configurations were tested, ranging from P = 17% to 42.24 % (Figure 2). Two configurations had openings equally distributed on the building height (P = 17 and 34 %), while two had a higher concentration of openings in the bottom part, simulating the presence of shops or hotels' foyers (P = 31.34 and 42.24 %). Hammer tests revealed, in the x-direction, an Eigen frequency of 41.5 Hz for the impervious configuration and 41.9 to 42.3 Hz for those with openings. These buildings were obtained by assembling aluminium plates with a thickness of 0.01 m, resulting into stiffness values of $1.69 - 1.15 \cdot 10^7$ N/m (model scale). Please note that two internal horizontal plates were constantly installed to simulate inner floors (Figure 2b).

Five Ultrasonic distance Sensors (US) captured the main characteristics of the propagating waves and the key features of the impact. These were located at x = 2.0, 10.1, 12.1, 13.35 and 13.85 m from the channel inlet, as detailed in Figure 1. The US were produced by Baumer Switzerland, model UNAM 30I6103, with a precision of ±0.5 mm and response time of 80 ms, resulting into an acquisition frequency of 12.5 Hz. These provided an average over a surface of 0.011 m^2 (r = 50 mm) within a measuring range of 100 to 1000 mm.

Two GoPro video cameras with a recording speed of 30 fps were positioned facing the upstream and downstream sides of the building, allowing to capture the main features of the impact.

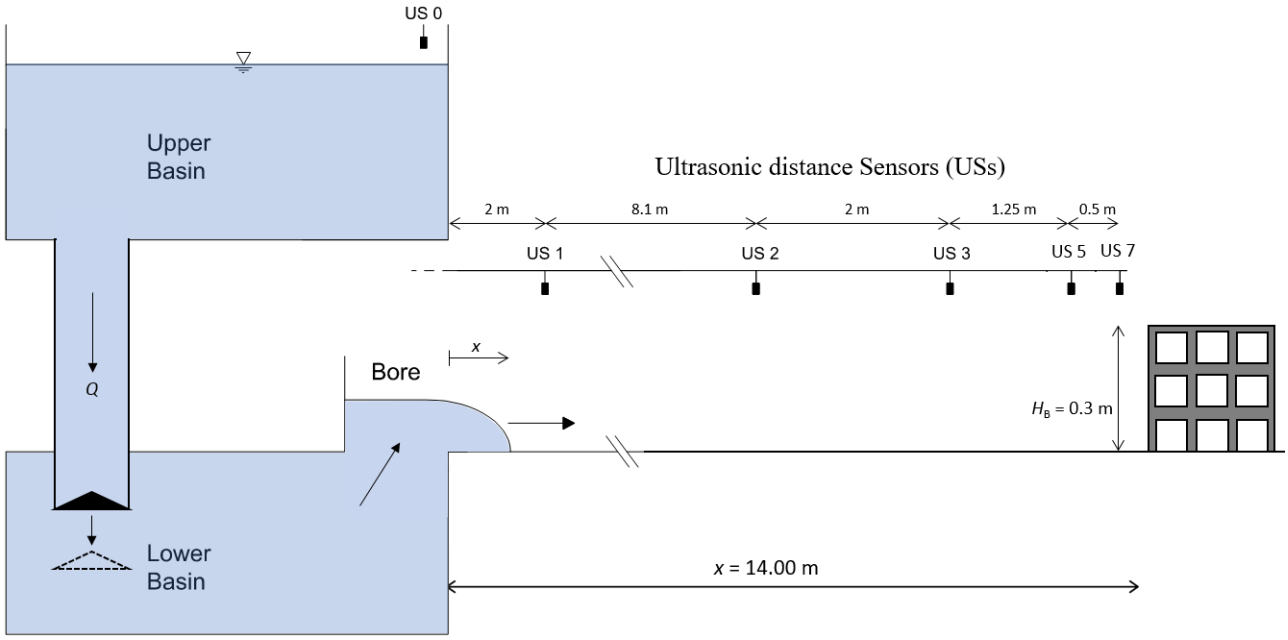

Figure 1. Experimental set-up

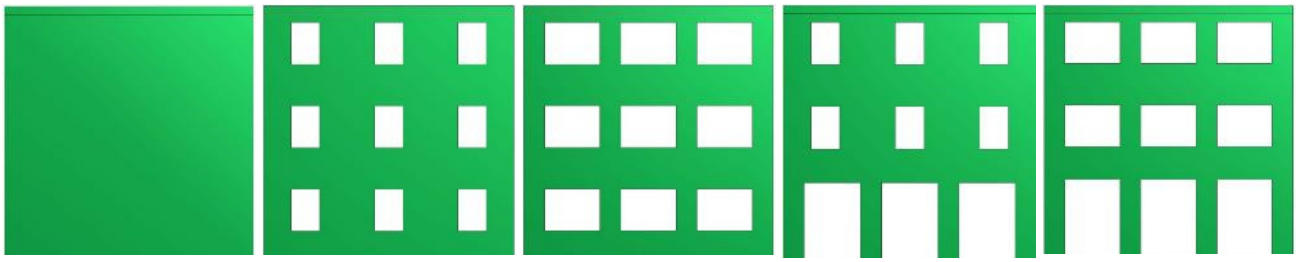

(a)

Configuration 0 (P = 42.24 %) Configuration F (P = 42.24 %)

(b)

Figure 2. Tested scenarios: (a) porosity values: (b) building configurations.

2.2 Numerical simulation model

Three-dimensional (3D) simulations employed a dam-break system for generating tsunami-like waves and were carried out by using SPH method that discretises the fluid flow field with explicitly tracked reference particles (Monaghan, 1992). Each particle has a smooth kernel function characterized by spatial distance denoted as "*smoothing length*." In this research, Wendland's function was used as the kernel function W_{ij} with smoothing length l:

$$W_{ij}=\frac{21}{16\pi l^2}\left(1-\frac{|r_{ij}|}{2l}\right)^4\left(\frac{2|r_{ij}|}{l}+1\right), \quad 0\le|r_{ij}|\le 2l \qquad [1]$$

$$\nabla_i W_{ij} = \frac{105}{16\pi l^5}\left(\frac{|r_{ij}|}{2l} - 1\right)^3 \boldsymbol{r}_{ij} \quad [2]$$

where $\boldsymbol{r}_{ij}$ is the position of particle i relative to particle j, r_k denotes the position of particle k, and $\nabla_i W_{ij}$ is the gradient of the kernel function.

Discretization of the Navier–Stokes equation of fluid with the kernel function allows the momentum and continuity equations to be expressed as

$$\frac{\mathrm{d}\boldsymbol{v}_i}{\mathrm{d}t} = -\sum_j m_j\left(\frac{p_j}{\rho_j^2} + \frac{p_i}{\rho_i^2}\right)\nabla_i W_{ij} + \sum_j m_j\left(\frac{v_i + v_j}{\rho_i + \rho_j}\cdot\frac{2\boldsymbol{r}_{ij}\cdot\nabla_i W_{ij}}{\boldsymbol{r}_{ij}^2 + \eta^2}\right)\boldsymbol{v}_{ij} \quad [3]$$

and

$$\frac{\mathrm{d}\rho_i}{\mathrm{d}t} = \sum_j m_j \boldsymbol{v}_{ij}\nabla_i W_{ij} \quad [4]$$

respectively, where v_{ij} is the relative velocity of particle i relative to particle j, and v_k, p_k, ρ_k, v_k, and m_k are the velocity, pressure, density, effective local viscosity, and mass of the k-th particle, respectively. η is a small parameter (set to $0.01l$) used for smoothing out the singularity at $r_{ij} = 0$. The local pressure in the first term on the right-hand side of Eq. (3) is given by the following equation of state, which is based on Tait's equation (Monaghan, 1994):

$$p_i = \frac{c_0^2\rho_0}{7}\left[\left(\frac{\rho_i}{\rho_0}\right)^7 - 1\right] \quad [5]$$

where ρ_0 is the reference density (1000 kg/m^3 of water), and c_0 is the speed of sound at the reference density. Thus, in the above model, fluid is treated as weakly compressible. Here, we determined 125 m/s as c_0 considering the computational cost. The second term on the right-hand side of Eq. (3) is the viscous stress force, while the right-hand side of Eq. (4) is compressibility (calculated by the kernel function).

The eddy viscosity effect caused by turbulence can be often incorporated into the viscous stress term using a large eddy simulation (LES) model. In this model, turbulence eddy viscosity is represented by the Smagorinsky model:

$$v^{\mathrm{LES}} = (\mathrm{C_s}\Delta)^2|S| \quad [6]$$

where C_s is a constant most often equal to 0.17, S is the strain rate tensor, and Δ is the LES filter size (taken equal to the kernel smoothing length l in SPH). Therefore, the local effective viscosity v can be expressed as a sum of kinematic viscosity v^{K} (1 μm^2/s of water) and turbulence eddy viscosity v^{LES}.

In this simulation using a dam-break system, we used a smooth horizontal channel with a length of 25.5 m and a width of 1.4 m, which is including a reservoir. Initial water mass was held in a reservoir with a length of 10 m and an initial impoundment depth of d_0 corresponding to a vertical release typed experimental set-up. The spatial resolution of the computation was set to 0.005 m as the SPH particle size, and the smoothing length l was chosen to be 2.1 times larger than the particle size to solve wave propagation with sufficient accuracy. In this setup, depending on the initial water depth, the number of SPH particles in the water mass can reach 90 million, which makes the cost of computation very high. Therefore, we used highly effective parallel computing techniques (Furuichi and Nishiura, 2017) to simulate wave propagation on a long-term scale of 15 s and employed a long channel length of 25.5 m. As a result, the computational time could be reduced to ~5 days by using 512 central processing unit nodes of the K super computer (RIKEN) in Kobe, Japan.

3 METHODOLGY

A number of 14 experimental tests performed by Wüthrich (2018) was selected for comparison with the numerical simulations. Details of these tests are presented in Table 1, along with the main hydrodynamic properties of the generated surges and bores. This work focused on a dry bed surge and wet bed bores with a release discharge corresponding to a dam-break wave with an initial impoundment depth of d_0 = 0.63 m (Wüthrich et al. 2018a). All data derived from the experimental work was obtained as the average of the available number of repetitions.

Table 1. Test program and wave main properties.

Impoundment depth [m]	Wave height [m]	Celerity [m/s]	Bed condition	Building porosity [%]	Building configuration	Experimental repetitions
0.63	0.162	3.114	Dry	0.00	0	4
0.63	0.224	2.437	Wet (0.05 m)	0.00	0	5
0.63	0.224	2.437	Wet (0.05 m)	17.00	0	1
0.63	0.224	2.437	Wet (0.05 m)	31.34	0	1
0.63	0.224	2.437	Wet (0.05 m)	34.00	0	1
0.63	0.224	2.437	Wet (0.05 m)	42.24	0	1
0.63	0.224	2.437	Wet (0.05 m)	42.24	F	1

4 RESULTS

These preliminary results focus on the inundation depths and specific features of the flow through the buildings, fundamental for the design of vertical shelters in tsunami prone areas. Initially the main hydrodynamic properties of the dry bed surges and wet bed bores are discussed, both experimentally and numerically. Afterwards, the impervious building is considered and finally the configurations with openings.

4.1 Wave Profiles

A detailed comparison of the SPH numerical simulations with the experimental data for both dry bed surges and wet bed bores was carried out by Nishiura et al. (2019). The difference in physical behaviour between a surge and a bore is well established in literature and visualized in Figure 3. Dry bed surges are characterized by a thin wave front, followed by a gradual rise in flow depth (Figure 3a,b). These are also associated with a higher front celerity, whereas wet bed bores are slower, but present a sudden rise in flow depth in the form of a turbulent aerated roller (Figure 3d,e). The SPH numerical simulations were able to capture such difference and the agreement between the two approaches is presented in Figure 3b and 3e. For surges, because of the thin shape of the propagating front, the spatial resolution of computation became insufficient and a simulation error was observed, thus explaining the single droplets in Figure 3b (Nishiura et al. 2019). For wet bed bores, one can notice some disagreement for the front profile (Figure 3f), due to the limitations of the numerical code, which does not take into account the turbulent and bubbly nature of the roller. Nishiura et al. (2019) also showed good agreement between numerical and experimental tests in terms of wave front celerity and longitudinal profiles, in agreement with those predicted by the theories of Ritter (1892) and Stoker (1957), not presented herein. Overall, Figure 3 shows the suitability of the SPH numerical simulations to reproduce tsunami-like flows that can therefore be used to simulate the impact on buildings.

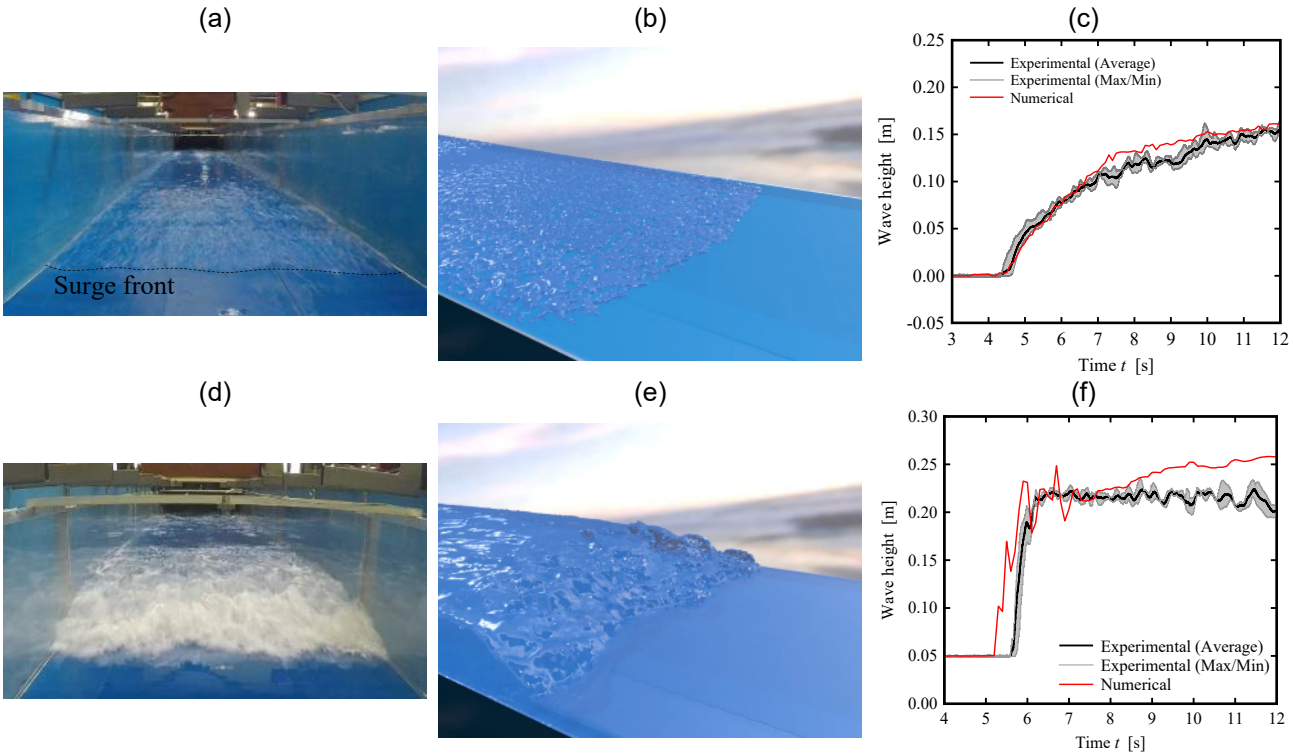

Figure 3. Comparison of numerical simulations and experimental tests for a dry bed surge (d_0 = 0.63 m) and a wet bed bore (d_0 = 0.63 m, h_0 = 0.05 m)

 ISSN 2521-7119 (Print) – ISSN 2521-716X (Online) – ISSN 2521-7127 (UBS)

4.2 Impervious building

Surges and bores described in section 4.1 are herein used to generate the impact on an impervious free-standing building (P = 0%, Figure 2). Consistently with previous studies, the process was characterised by two main phases: (1) a short initial impact phase (Figure 4a, c), followed by (2) a longer hydrodynamic phase with sustained upstream water depths (Figure 4b, d). The SPH numerical simulation was visually able to well reproduce the key features of the flow during and after the impact onto the impervious building for both the dry bed surge and the wet bed bore (Figure 4). Some differences can be observed in terms of air entrainment, as the aeration process is not taken into account in the numerical simulations. Some minor overflow of the building is observed in during the hydrodynamic phase of the impact.

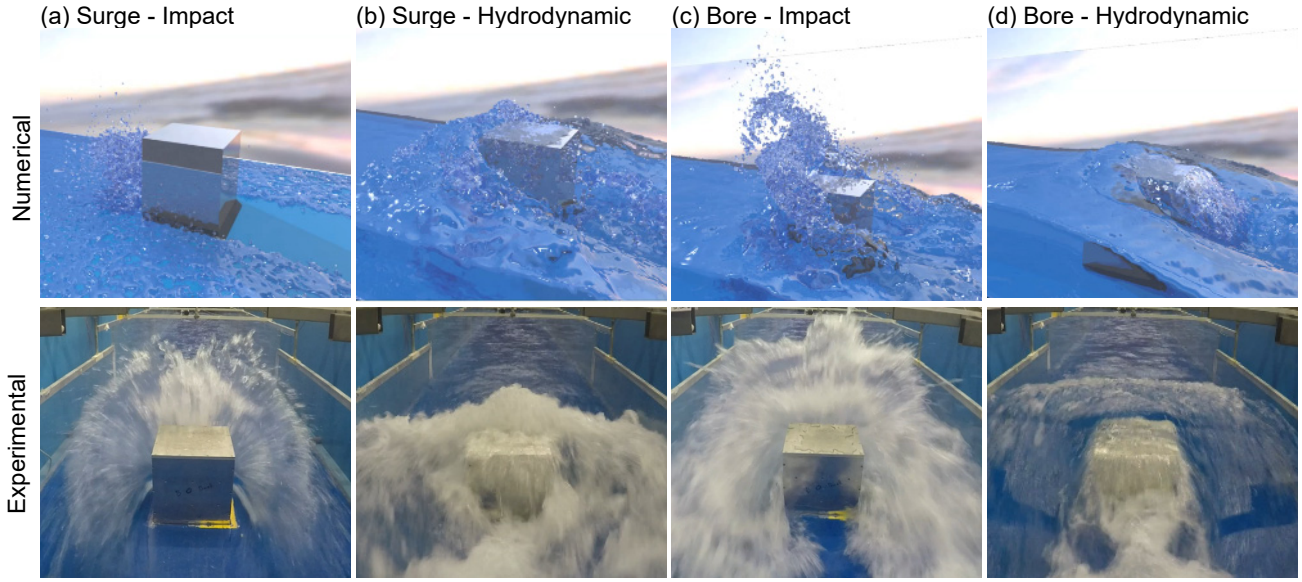

Figure 4. Comparison of numerical simulations (top) with experimental tests (bottom) during the wave impact of a dry bed surge (d_0 = 0.63 m) and a wet bed bores (d_0 = 0.63 m, h_0 = 0.05 m).

For a better insight of the process, the water depths on the upstream side of the building were recorded using two US sensors located 0.15 and 0.65 m upstream of the building. (US5 and US7, Figure 1). These values, averaged over a circular surface with a diameter of 5 cm, are compared to the numerical simulations in Figure 5. For the dry bed surge, a difference in arrival time can be observed, attributed to the insufficient number of particles to capture the wave front region, where the thin flow depths require a finer resolution. Furthermore, an underestimation of impact run-up heights is constantly observed for the numerical simulations, as compared to the experimental tests. Better agreement was found during the impact of a wet bed bore (Figure 5b), even if the effect of aeration is herein not considered. Nevertheless, despite these differences in the impact phase, similar flow depths are observed during the sustained hydrodynamic phase (t > 7-8 s) for both configurations.

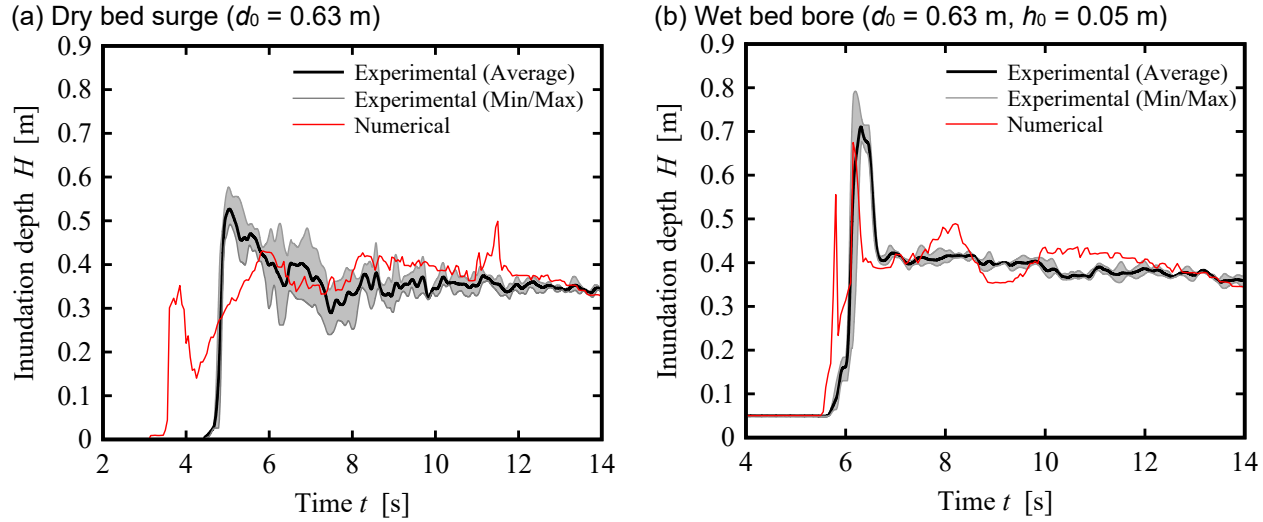

Figure 5. Comparison of inundation depths on the upstream side of the impervious building (x = 13.85, US7) for a dry bed surge (d_0 = 0.63 m) and a wet bed bore (d_0 = 0.63 m, h_0 = 0.05 m).

4.3 Building openings

The wet bed bore presented in section 4.1 was herein used to generate the impact on buildings with different porosities and configurations (Table 1, Figure 2, 3). Experimentally, the presence of openings induced a flow thought the building which changed the dynamics of the impact and the hydrodynamic phase. Figure 6 presents a sequence of the bore impact on a porous building with openings equally distributed on all four sides (P = 42.24%, Configuration 0). One can note that the initial impact is followed by a steadier flow through and around the building, consistently with the observations for the impervious building. As detailed in Figure 6, the numerical simulation was able to capture these main features and correctly reproduce the complex flow through the building. In agreement with the results for the impervious configuration, major differences in terms of air entrainment are observed on the upstream side of the building, where the recirculating roller is not correctly reproduced. The numerical simulations also point out an increase of the downstream water depths associated with the flow through the openings. This was previously pointed out to be a key feature in the reduction of the total horizontal forces acting on the building (Wüthrich et al. 2018c).

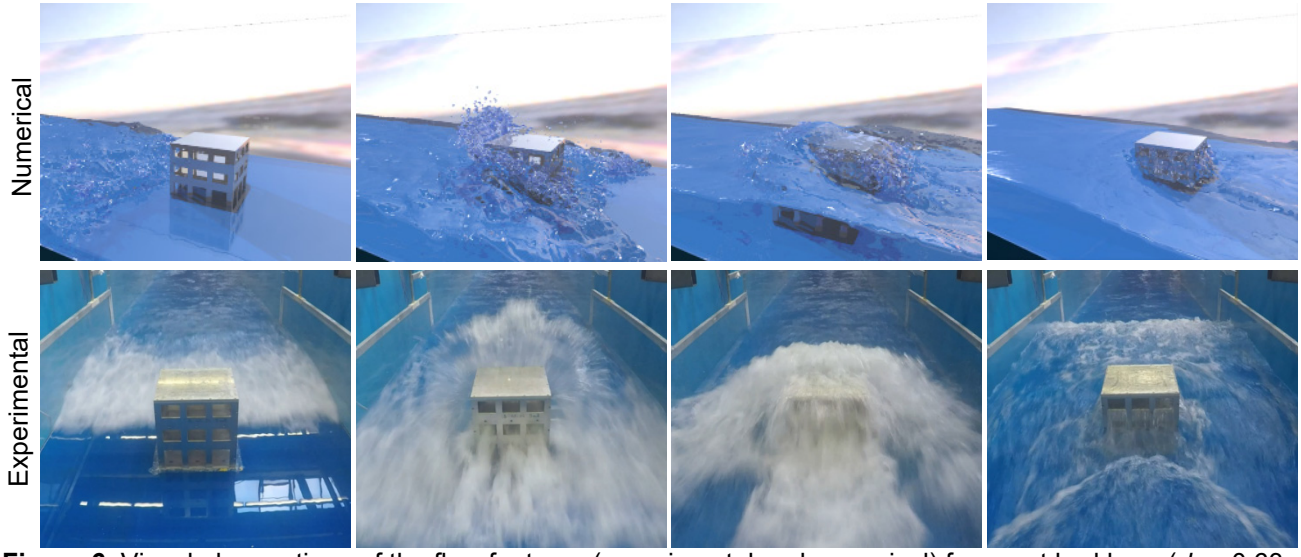

Figure 6. Visual observations of the flow features (experimental and numerical) for a wet bed bore (d_0 = 0.63 m, h_0 = 0.05 m) impacting on a porous building (P = 42.24%, Configuration 0).

The water depths recorded on the upstream side of the building (US5 and US7 in Figure 1) showed some good agreement between the experimental tests and the numerical simulations. For all configurations with openings, similar impact run-up heights were captured at x = 13.85 m, as shown in Figure 7a (5 s < t < 7 s). In addition, one can recognise consistent behaviours in the hydrodynamic phase, where differences are attributed to the incorrect representation of the roller in the numerical simulations (t > 7-8 s). The US5 located 0.65 m upstream of the building was less affected by the recirculating roller and impact splashes, thus providing a better characterization of the upstream inundation depths. The constriction due to presence of the building within the channel resulted into a change in the flow regime, generating waves propagating in the upstream direction. These took place earlier in the numerical simulations, probably associated to the turbulent and recirculating nature of the roller. Nevertheless, Figure 7b shows a good agreement between the numerical simulations and experimental data in the computation of the inundation depths.

The effect of openings on the side walls was also investigate both numerically and experimentally (Figure 7c). Wüthrich et al. (2018c) previously showed that for highly unsteady flows, no major differences were observed between these two configurations in terms of upstream water depths. However, impervious sidewalls prevented any water exchange in the transversal direction, thus resulting into a more uniform flow around the building. The upstream water depths for both configurations 0 and F for P = for 42.24 % are compared in Figure 7c, where the numerical simulation generated slightly higher flow depths for the configuration with impervious sidewalls (F), most likely associated with the different turbulent nature of the impact. Nevertheless, in the upstream measurement location (US5) unaffected by the recirculating roller, no remarkable differences can be observed, in agreement with the experimental results.

 ISSN 2521-7119 (Print) – ISSN 2521-716X (Online) – ISSN 2521-7127 (UBS)

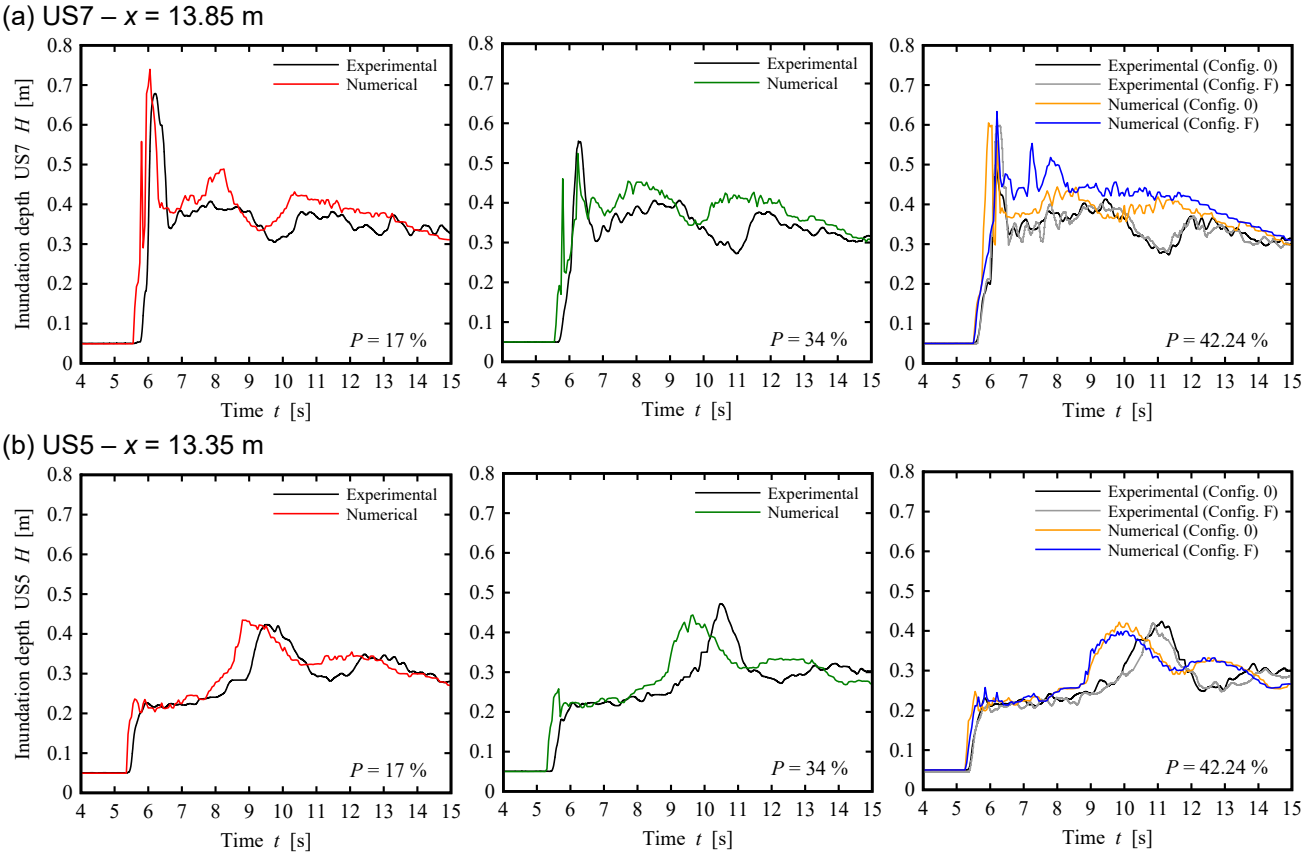

Figure 7. Comparison of inundation depths on the upstream side of the building (US7 and US5) for the configurations with openings.

5 CONCLUSIONS

Unsteady flows such as tsunamis, impulse waves and dam-break waves are responsible for damages to infrastructures and human losses, thus pointing out the need for specific research. For a more comprehensive understating of the process, a hybrid approach combining experimental tests with numerical simulations is essential. This study focused on the validation of SPH numerical simulations performed using highly effective parallel computing techniques with large-scale experiments for the impact of waves on buildings with and without openings. Because of their different physical behaviour, this study investigated both dry bed surges and wet bed bores during their impact on free-standing buildings. The thin nature of the surge front led to some computational instabilities, thus pointing out the need for a higher spatial resolution and a more comprehensive model taking into account turbulence and air entrainment. Although preliminary, these current results showed a good agreement between the two approaches in the reproduction of inundation depths during tsunami-like events. Despite some discrepancies during the impact phase, similar values were found in the sustained hydrodynamic phase for both impervious and porous configurations. The effect of aeration remains difficult to assess and further implementations are necessary. In agreement with experimental data, the numerical simulations were able to capture the main features of the flow through the buildings, resulting into higher upstream water depths, responsible for the lower loads induced on the structure. Although encouraging, these results stressed the need for further improvement of the numerical simulations and future work will include a comparison of the forces and moments acting on the building. This will support the development of a useful practical tool to predict inundation depths and structural loads, necessary for a safer design of hydraulic structures.

ACKNOWLEDGEMENTS

This research was conducted as part of the ENATIS project (Experimental-Numerical Approach for Tsunami Impact on Structures) cofounded by LCH-EPFL and JAMSTEC. The supports of the Swiss National Science Foundation (SNSF) [grants grant number 200021_149112/1 and 200021_149112/2], the Earth Simulator project of JAMSTEC, MEXT as “Priority Issue on Post-K computer” (System for Integrated Simulation of Earthquake and Tsunami Hazard and Disaster) using computational resources of the K computer provided by the RIKEN Centre for Computational Science through the HPCI System Research project (Project ID: hp180207, “Joint Usage/Research Centre for Interdisciplinary Large-scale Information Infrastructures”, and “High Performance Computing Infrastructure” in Japan (Project ID: jh180060-NAH, jh180065-NAH) are acknowledged.

REFERENCES

Arnason, H., Petroff, C. and Yeh, H. (2009). Tsunami Bore Impingement onto a Vertical Column. *Journal of Disaster Research* 4 (6): 391–403.

Asadollahi, N., Nistor, I., and Mohammadian, A. (2018a). Numerical investigation of tsunami bore effects on structures, part I: drag coefficients. *Nat. Haz.*, 1-25.

Asadollahi, N., Nistor, I., and Mohammadian, A. (2018b). Numerical investigation of tsunami bore effects on structures, part II: effects of bed condition on loading onto circular . *Nat. Haz.*, 1-21.

Chanson, H. (2006). Tsunami surges on dry coastal plains: Application of dam break wave equations, *Coastal Eng. J.*, 48 (4), 355–370.

Chanson, H., Aoki, S.I., and Maruyama, M. (2002). Unsteady air bubble entrainment and detrainment at a plunging breaker: Dominant time scales and similarity of water level variations. *Coastal Eng.*, 46 (2), 139–157.

Chock, G., Robertson, I., Kriebel, D., Francis, M. and Nistor, I. (2012). Tohoku Japan Tsunami of March 11, 2011 – Performance of Structures, 348. *American Society of Civil Engineers* (ASCE).

Crespo, A.J., Dominguez, J.M., Rogers, B.D., Gomez-Gesteira, M., Longshaw, S., Canelas, R., Vacondio, R., Barreiro, A. and Garcia-Feal, O. (2015). DualSPHysics: Open-source parallel CFD solver based on Smoothed Particle Hydrodynamics (SPH). *Comput. Phys. Comm.*, 187, 204–216.

Cross, R. (1967). Tsunami Surge Forces. *Journal of the Waterways and Harbors Division,* 93 (4), 201–231.

Foster, A.S.J., Rossetto, T., and Allsop, W. (2017). An Experimentally Validated Approach for Evaluating Tsunami Inundation Forces on Rectangular Buildings, *Coastal Eng.*, 128, 44–57.

Furuichi, M. and Nishiura, D. (2017). Iterative Load-Balancing Method with Multigrid Level Relaxation for Particle Simulation with Short-Range Interactions. *Comput. Phys. Comm.*, 219, 135–148.

Guler, H.G., Baykal, C. Arikawa, T. and Yalciner, A.C. (2018). Numerical assessment of tsunami attack on a rubble mound breakwater using OpenFOAM (R). *Appl. Ocean Res.*, 72, 76–91.

Madsen, P. A., Fuhrman, D. R., and Schäffer, H. A. (2008). On the solitary wave paradigm for tsunamis. *J. Geophys. Res. C: Oceans*, 113, 1–22.

Meile, T., Boillat, J.L., and Schleiss, A.J. (2011). Water-surface oscillations in channels with axi-symmetric cavities, *J. Hydraul. Res.*, 49 (1), 73-81.

Monaghan, J.J. (1992). Smoothed Particle Hydrodynamics. *Annu. Rev. Astron. Astrophys.*, 30, 543–574.

Monaghan, J.J. (1994). Simulating Free Surface Flows with SPH. *J. Comput. Phys.*, 110 (2), 399–406.

Nishiura, D., Furuichi, M. and Sakaguchi, H. (2015). Computational Performance of a Smoothed Particle Hydrodynamics Simulation for Shared-Memory Parallel Computing. *Comput. Phys. Comm.*, 194, 18–32.

Nishiura, D., Wüthrich, D., Furuichi, M., Nomura, S., Pfister, M. and De Cesare, G. (2019). Numerical Approach in the Study of Tsunami-like Waves and Comparison with Experimental Data. *Proc. of the 29th Int. Ocean & Polar Eng. Conf. (ISOPE 2019)*, Honolulu, HI, USA, 16-21 June.

Nouri, Y., Nistor, I., Palermo, D., and Cornett, A. (2010). Experimental Investigation of the Tsunami Impact on Free Standing Structures, *Coastal Eng. J.*, 52 (1), 43-70.

Ramsden, J.D. (1993). Tsunami: Forces on a Vertical Wall Caused by Long Waves, Bores, and Surges on a Dry Bed, *Ph.D. Thesis*, California Institute of Technology, Pasadena, CA.

Ritter, A. (1892). Die Fortpflanzung der Wasserwellen, *Zeitschrift des Vereins Deutscher Ingenieure*, 36, 947–954.

Rossetto, T., Allsop, W., Charvet, I., and Robinson, D. (2011). Physical modelling of tsunami using a new pneumatic wave generator, *Coastal Eng.*, 58 (6), 517–527.

Shafiei, S., Melville, B.W., and Shamseldin, A.Y. (2016). Experimental investigation of tsunami bore impact force and pressure on a square prism, *Coastal Eng.*, 110, 1–16.

St-Germain, P., Nistor, I., Townsend, R., and Shibayama, T. (2014). Smoothed-Particle Hydrodynamics Numerical Modeling of Structures Impacted by Tsunami Bores, *J. Waterway, Port, Coastal, Ocean Eng.*, 140 (1), 66–81.

Stoker, J.J. (1957). *Water waves: The mathematical theory with applications*, John Wiley& Sons.

Thusyanthan, N. and Madabhushi, S. (2008). Tsunami wave loading on coastal houses: a model approach. *Civ. Eng.*, 161 (2), 77– 86.

Triatmadja, R. and Nurhasanah, A. (2012). Tsunami force on buildings with openings and protection. *Journal of Earthquake and tsunami*, 6 (4), 1250024.

Wilson, J., Gupta, R., Van de Lindt, J., Clauson, M. and Garcia, R., (2009). Behavior of a one-sixth scale wood-framed residential structure under wave loading. *J. Perform. Constr. Facil*. 23 (5), 336 – 345.

Wüthrich D., Chamoun S., Bollaert E., De Cesare G. and Schleiss A.J. (2018) Hybrid modelling approach to study scour potential at Chancy-Pougny dam stilling basin. *Advances in Hydroinformatics*, Springer Water, Singapore, pp. 869-884.

Wüthrich, D. (2018). Extreme hydrodynamic impact onto buildings. *EPFL PhD Thesis* (N. 8116) and LCH Communication n.74, Lausanne, Switzerland, 246 pages.

Wüthrich, D., Pfister M., Nistor, I. and Schleiss, A.J. (2018a). Experimental Study of Tsunami-Like Waves Generated with a Vertical Release Technique on Dry and Wet Beds. *J. Waterway, Port, Coastal, Ocean Eng.*, 144 (4), 04018006.

Wüthrich, D., Pfister M., Nistor, I. and Schleiss, A.J. (2018b). Experimental study on the hydrodynamic impact of tsunami-like waves against impervious free-standing buildings. *Coast. Eng. J.*, 60 (2), 180-199.

Wüthrich, D., Pfister M., Nistor, I. and Schleiss, A.J. (2018c). Experimental study on forces exerted on buildings with openings due to extreme hydrodynamic events. *Coastal Eng*., 140, 72-86.

Wüthrich, D., Pfister M., Nistor, I. and Schleiss, A.J. (2019). Effect of building's overtopping on induced loads during extreme hydrodynamic events. *J. Hydraul. Res.* (published online).

Ylla Arbós, C., Wüthrich, D., Pfister, M. and Schleiss, A.J. (2018). Wave impact on oriented impervious buildings. *Proc. of the 5th IAHR Europe Congress*, Trento, Italy, 13-15 June, pp. 791-792.